



Research Paper

Estimating Pier Scour Depth: Comparison of Empirical Formulations with ANNs, GMDH, MARS, and Kriging

Moslem Zarbazoo Siahkali¹, Abbasali Ghaderi¹, Abdolhamid Bahrpeyma^{1*}, Mohsen Rashki² and Naser Safaeian Hamzehkolaei³

1. Department of Civil Engineering, University of Sistan and Baluchestan, Zahedan, Iran.

2. Department of Architecture Engineering, University of Sistan and Baluchestan, Zahedan, Iran.

3. Department of Civil Engineering, Bozorgmehr University of Qaenat, Qaen, Iran.

Article Info

Article History:

Received 26 September 2020

Revised 27 October 2020

Accepted 21 December 2020

DOI:10.22044/jadm.2020.10085.2147

Keywords:

Pier Scour, Surrogate Models, Artificial Neural Networks, Kriging, Sensitivity Analysis.

*Corresponding author:
bahrpeyma@arts.usb.ac.ir (A. Bahrpeyma).

Abstract

Scouring, occurring when the water flow erodes the bed materials around the bridge pier structure, is a serious safety assessment problem for which there are many equations and models available in the literature in order to estimate the approximate scour depth. This research work is aimed to study how the surrogate models estimate the scour depth around circular piers, and compare the results with those of the empirical formulations. To this end, the pier scour depth is estimated in non-cohesive soils based on a sub-critical flow and live bed conditions using the artificial neural networks (ANNs), group method of data handling (GMDH), multivariate adaptive regression splines (MARS), and Gaussian process models (Kriging). A database containing 246 lab data gathered from various studies is formed, and the data is divided into three random parts: 1) training, 2) validation, and 3) testing in order to build the surrogate models. The statistical error criteria such as the coefficient of determination (R^2), root mean squared error (RMSE), mean absolute percentage error (MAPE), and absolute maximum percentage error (MPE) of the surrogate models are then found and compared with those of the popular empirical formulations. The results obtained reveal that the surrogate models' test data estimations are more accurate than those of the empirical equations; Kriging has better estimations than the other models. In addition, the sensitivity analyses of all the surrogate models show that the pier width's dimensionless expression (b/y) has a greater effect on estimating the normalized scour depth (D_s/y).

1. Introduction

The bridge pier local scour, which is a vital limiting factor involved to assign the minimum substructure depth, is the removal of the river bed materials from around the pier foundation. This issue is important because if the scour depth is overestimated, the result will be an increased foundation depth, and an increased pier base design depth, and hence, the increased project implementation costs; and if it is underestimated, there will be an increased bridge destruction risk. Shirhole and Holt [1] believed that the bridge failure due to hydraulic factors (scour, ice, and

debris) was more serious compared to the other factors involved (overloading, collision, structural details, earthquake, etc.). Therefore, a correct estimation of this phenomenon is a very effective parameter in bridge safety evaluations. However, due to the natural complexity of the phenomenon and thus its modeling, many researchers such as Breusers et al. [2], Melville & Coleman [3], Richardson & Davis [4], and Sheppard & Miller [5] studied the case and proposed different empirical relations based on a specific dataset and different input variables. The important point is

that most of the existing models do not yield a proper estimation accuracy, and often provide different, highly conservative, and overestimated scour depths. Therefore, their estimations of the maximum scour depth are not satisfactory, and their use in the design of real-world cases is unreliable since it generally leads to higher foundation design costs [6].

Since different sources have stated that a single reliable equation does not exist in order to estimate the scour depth for various ranges, alternative methods (e.g. surrogate modeling) have been widely used, and have become effective tools to provide more accuracy in the hydraulic design problems. Although they have performed much better than the methods that are mostly regression-based, some of them cannot provide an explicit relation between the scour depth and its decision variables [7, 8].

ANNs, MARS, GMDH, and Kriging find relations between a set of effective variables as the model inputs and the local scour depth as the target variable. Many studies have shown the efficiency of these methods in the engineering problems, and many researchers ([9-13]) have used them successfully to solve the hydraulic problems.

In order to estimate the scour depth, the researchers have used different ANNs, GMDH, MARS, and Kriging models. Bateni et al. [7] have applied MLP/BP (multi-layer perception) and RBF/OLS (radial basis) (two ANN models) along with ANFIS (adaptive neuro-fuzzy inference system) and numerous lab data in order to estimate the scour depth around bridge piers by modeling the equilibrium scour depth as a function of five variables including the flow depth, mean velocity, critical flow velocity, mean grain diameter, and pier diameter. In order to check the estimation accuracy of the mentioned models, their results have been compared with those of 8 other empirical relations, and it has been confirmed that the proposed approaches are much more accurate in estimating the scour depth. Firat and Gungor [14] have studied the ANN's ability in order to estimate the scour depth around circular bridge piers, have compared the results obtained with those of the empirical formulae, and have shown that the Generalized Regression Neural Network (GRNN) model can not only do the task successfully but is also more reliable and accurate.

Najafzadeh et al. [15] have compared the results of the GMDH network and the traditional equations for estimation of the scour depth in

cohesive soils, proving that the former is much more successful than the latter.

Bateni et al. [8] have utilized the GEP (genetic expression programming) and MARS models in order to estimate the equilibrium scour depth around pile groups; they compared their performance with those of the empirical equations and showed that they could estimate the equilibrium scour depth more accurately than the existing equations; MARS was more accurate than GEP.

The studies that have evaluated the performance of these models in order to estimate the scour depth are numerous; however, Kriging has not been widely used so far in this domain. In order to show its capabilities in other fields, Qin et al. [16] have successfully applied a hybrid Kriging model-genetic algorithm to modify the FEM (finite element method) analyses of complex bridge structures, showing that the Kriging surrogate model performed well in estimating the structural response and reducing the computational costs. Fan et al. [17] have examined if the Kriging surrogate models could optimally design crane-bridge systems based on reliability, showing that it could considerably improve the computational efficiency with a good accuracy. Lu et al. [18] have used the Kriging model in order to estimate the bridge static load, showing that Kriging has a good accuracy, and the results obtained conform well to those of the static load tests. Therefore, the above-mentioned studies and their results show that the performance and effectiveness of the proposed method are acceptable for the estimation or optimization purpose.

In this work, we investigated the efficiency of the Kriging model in comparison with the GMDH, ANN, and MARS models, and some existing traditional equations in order to estimate the pier scour depth under live bed conditions with uniform sediments in non-cohesive soils considering the influence of the effective parameters on the performance of the surrogate models to estimate the scour depth.

2. Local Scour Around a Pier and Data Collection

Soil materials are eroded from around bridge piers or other hydraulic structures built in flowing water. Since this sediment removal (also called local scouring) phenomenon, due to the flow-pier interaction (figure 1), is a main bridge-failure factor, because it undermines the foundation, we are required to precisely estimate the pier-vicinity scour hole in order to take the necessary measures to prevent the structure from erosion-related

failures all through its service life. Nevertheless, since the pier obstruction and sediment erosion, which form the scour hole, are complicated interactions between different fluid flow patterns and the scour affecting variables are many, making a dependable numerical/analytical model that can consider different inter-related controlling factors, without having to oversimplify the case, is not easy. The local scour depth estimation is not

possible by an accurate method; hence, empirical methods are used for this purpose since different designers have varied opinions and use different equations. Since this issue depends on such parameters as the fluid, flow, bed sediment, and pier geometry, many research works have been done by many colleagues in order to investigate the factors that affect the scour depth around bridge piers.

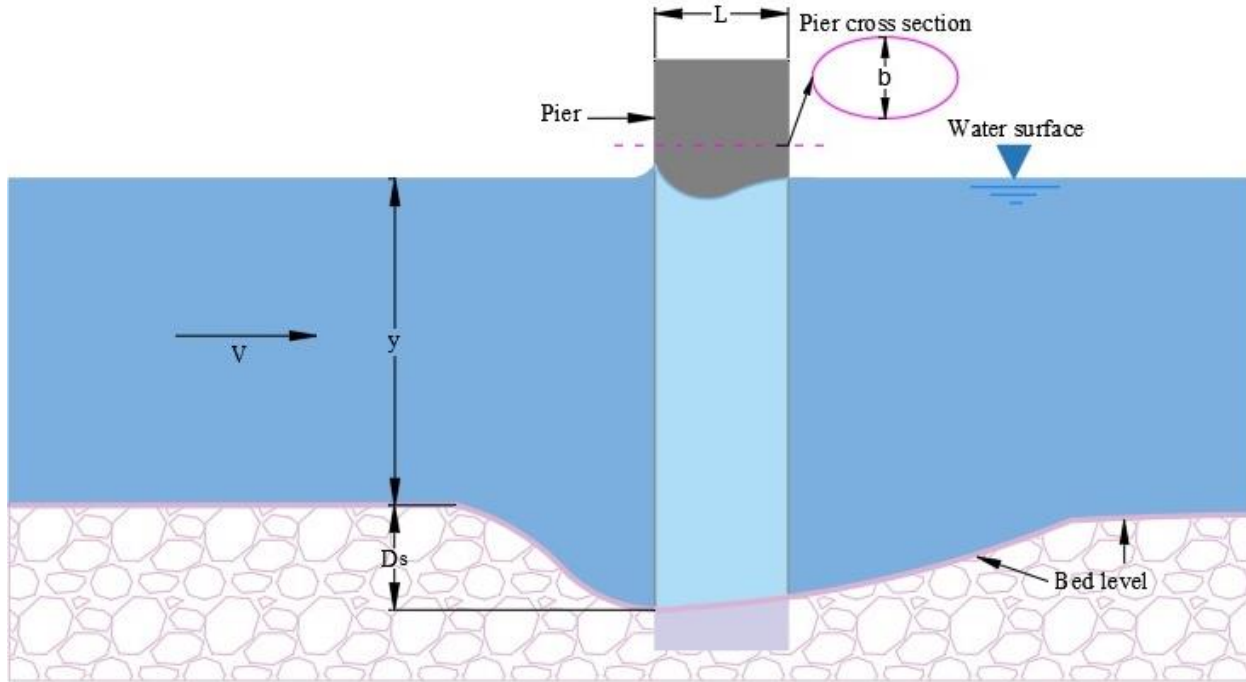


Figure 1. Sketch of local scour of pier.

After Azamathulla et al. [19] compared the GP performance with those of ANNs and regression equations and concluded that the former was more effective, they used it as an alternative to HEC-18 (conventional regression-based equations) in order to find the scouring of bridge piers.

They expressed the factors affecting the equilibrium scour depth at piers as a function of the following variables:

$$D_s = f(V, y, D_{50}, \sigma, b, L, g) \quad (1)$$

where V and y are the approach flow velocity and depth, respectively, D_{50} is the mean particle diameter, σ is the standard deviation of the grain size distribution, b and L are the pier width and length, respectively, and g is the gravity-caused acceleration.

Since the non-dimensional parameters yielded better scour depth estimations than the dimensional ones, some papers [20-22] analyzed models with a non-dimensional dataset and found the following equation with 5 decision variables using the dimensional analysis method:

$$\frac{D_s}{y} = f\left(F_r, \frac{b}{y}, \frac{D_{50}}{y}, \frac{L}{y}, \sigma\right) \quad (2)$$

where D_s/y , b/y , D_{50}/y , L/y , F_r , and σ are the scour depth, pier width, mean particle diameter, pier length (all non-dimensional), Froude number, and standard deviation of the grain size distribution, respectively.

Hence, the decision variables are, next, reduced as follows using the dimensional analysis technique:

$$D_s = f(V, y, D_{50}, \sigma, b, g) \quad (3)$$

Hence, using the circular-section piers in this work led to their equilibrium scour depth to be a function of the variables mentioned below:

$$\frac{D_s}{y} = f\left(F_r, \frac{b}{y}, \frac{D_{50}}{y}, \sigma\right) \quad (4)$$

The above parameters were used in order to develop the surrogate models and the results obtained were compared with those of four empirical equations in order to evaluate the efficiency of the developed models. The selected equations (table 1) included: 1) modified HN/GC [23], 2) Laursen and Toch [24], 3) Johnson [25], and 4) FHWA HEC-18 [26] (based on the Colorado State University 'CSU' Equation).

Tables 2 and 3 show the surrogate models developed for uniform sand bed materials using a

dataset of totally 246 cases, out of which 99 were reported by Chiew [27], 75 by Chabert and Engeldinger [28], 50 by Chee [29], 15 by Jain and Fischer [30, 31], and 7 by Chen [32], all gathered through observations of live bed scour ($V > V_c$)

and a sub-critical flow regime ($F_r < 1$). Since the armoring phenomenon would probably occur at $\sigma > 1.3$, lower values ($\sigma < 1.3$) were considered [33].

Table 1. Empirical methods used for comparison.

Reference	Equation	Notes
Laursen and Toch (1956)	$D_s = 1.35b^{0.7}y^{0.3}$	
Johnson (1992)	$D_s = 2.02y(\frac{b}{y})^{0.98}F_r^{0.21}\sigma^{(-0.24)}$	$\sigma = \frac{D_{84}}{D_{50}}$
CSU (1993)	$\frac{D_s}{y} = 2.0K_1K_2K_3K_4(\frac{b}{y})^{0.65}F_r^{0.43}$	$F_r = \frac{V}{\sqrt{gy}}$
modified HN/GC (2016)	$\frac{D_s}{b^{0.62}y^{0.38}} = 1.32K_1K_2K_3[\tanh(\frac{H^2}{1.97\sigma^{1.5}})]$	$H = \frac{V}{\sqrt{g(S_g)D_{50}}}$

where:

- D_s = Predicted pier scour depth;
- σ = Sediment gradation coefficient;
- F_r = Approach flow Froude number defined as
- H = Hager number (densimetric particle Froude number (F_r));
- b = Pier width;
- y = Approach flow depth;
- D_{84} = Sediment diameters for which 84% of the sediment material is finer;

- D_{50} = Median grain size;
- K_1 and K_2 = Correction coefficient pier nose shape and flow angle of attack, respectively. For a circular pier, both K_1 and K_2 are equal to one;
- K_3 = Correction factor for bed conditions (for clear water ($K_3 = 1.1$) and live bed ($1.1 \leq K_3 \leq 1.3$));
- V = Mean approach velocity;
- g = Gravitational acceleration
- S_g = Specific gravity of the sediment

Table 2. Data sources.

Source	Chiew (1984)	Chabert and Engeldinger (1956)	Chee (1982)	Jain and Fischer (1979,1980)	Chen (1980)	SUM
Number Of Data	99	75	50	15	7	246

Table 3. Range of data.

Parameters	Maximum	Average	Minimum	Std. Deviation
F_r	0.999	0.606	0.201	0.214
σ	1.28	1.185	1.094	0.048
D_{50}/y	0.035	0.008	0.0015	0.007
b/y	1.50	0.513	0.132	0.342
D_s/y	1.75	0.669	0.156	0.365

Figure 2 shows the input-output variable relationship assessed through the Pearson correlation analysis. Here, heatmaps represent the absolute values of the correlation coefficients. Those in yellow/pink mean strong

positive/negative inter-variable correlations. Since b/y has the highest correlation, $b/y-D_s/y$ has a strong positive linear relationship; that of other input-output variables is negligible.

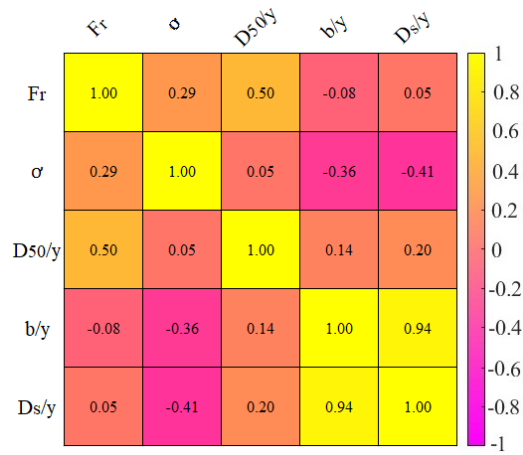


Figure 2. Heatmap of correlation between the input and output variables.

3. Surrogate Models and Statistical Performance Measures

Surrogate (Meta) models are used in order to simulate and find the relationships between the different input variables and how they affect the outputs in complex models. The general steps in building a surrogate model are: 1) Generating/defining its input parameters and their variation range, 2) Determining its structure/type, 3) Estimating its training parameters, and 4) Evaluating its performance [34].

Since the accuracy/success of these methods highly depends on the data points and sample

locations, the database was randomly divided (figure 3) into: 1) A training subset (with 172 data or 70%) to construct the surrogate model and avoid overfitting, 2) A validation subset (with 37 data or 15%) in order to evaluate the model’s generalization capability, check its performance throughout the training stage, and finally, determine the model’s optimum input parameters, and 3) A test subset (with 37 data or 15%) to evaluate the performance of the developed surrogate models through comparisons with the existing empirical equations.

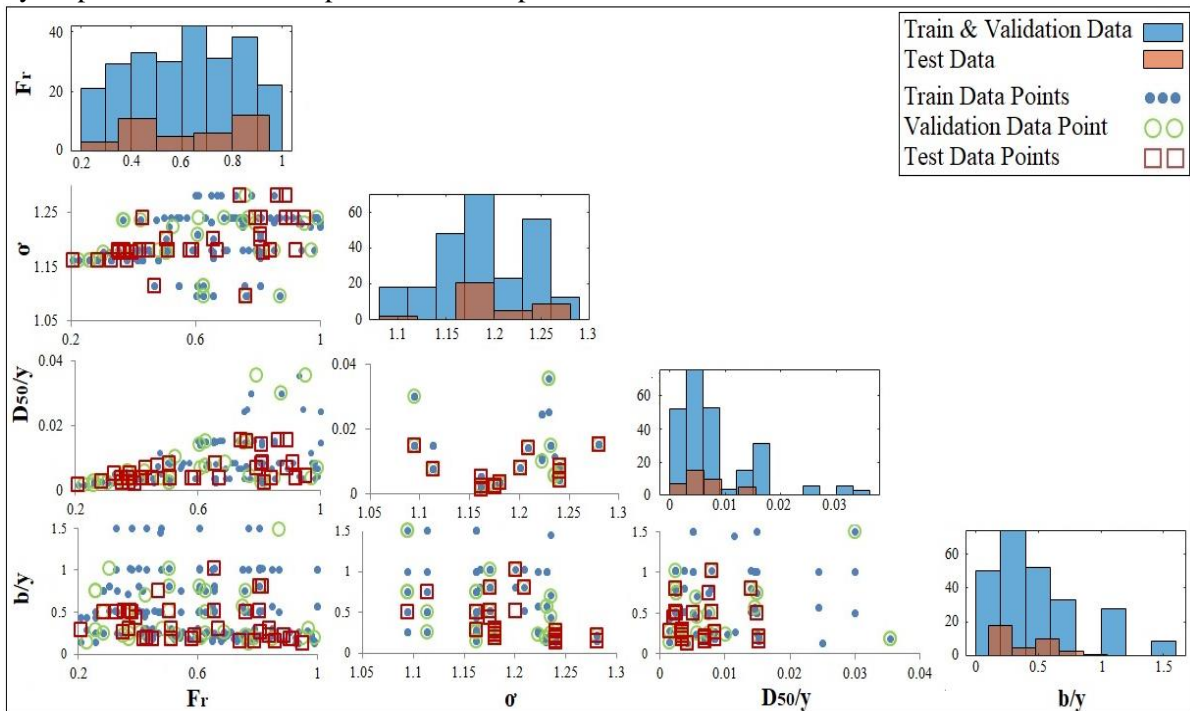


Figure 3. Properties of dataset used for estimating D_s/y .

In this work, we used the ANNs, GMDH, MARS, and Kriging techniques of the surrogate modeling in order to estimate the pier scour depth. Next, the RMSE (root mean square error), R^2 (coefficient of determination), MAPE (mean absolute percent

error), and MPE (maximum percent error) performance measures ((5)-(8)) were applied to compare each model’s accuracy/efficiency.

$$RMSE = \sqrt{\frac{1}{n} \sum_{i=1}^n \left(\left(\frac{D_s}{y} \right)_p - \left(\frac{D_s}{y} \right)_A \right)^2} \quad (5)$$

$$R^2 = \frac{\left[\sum_{i=1}^n \left(\left(\frac{D_s}{y} \right)_A - \overline{\left(\frac{D_s}{y} \right)_A} \right) \left(\left(\frac{D_s}{y} \right)_p - \overline{\left(\frac{D_s}{y} \right)_p} \right) \right]^2}{\left[\sum_{i=1}^n \left(\left(\frac{D_s}{y} \right)_A - \overline{\left(\frac{D_s}{y} \right)_A} \right)^2 \sum_{i=1}^n \left(\left(\frac{D_s}{y} \right)_p - \overline{\left(\frac{D_s}{y} \right)_p} \right)^2 \right]} \quad (6)$$

$$MAPE = \frac{1}{n} \sum_{i=1}^n \left| \frac{\left(\frac{D_s}{y} \right)_p - \left(\frac{D_s}{y} \right)_A}{\left(\frac{D_s}{y} \right)_A} \right| \quad (7)$$

$$MPE = \text{MAX} \left(\left| \frac{\left(\frac{D_s}{y} \right)_i - \left(\frac{D_s}{y} \right)_A}{\left(\frac{D_s}{y} \right)_A} \right| * 100 \right), \quad i = 1, 2, 3, \dots, n \quad (8)$$

where $\left(\frac{D_s}{y} \right)_A$ are the measured data, $\left(\frac{D_s}{y} \right)_P$ are the model estimations of the non-dimensional scour depth, n is the number of data points, and $\overline{\left(\frac{D_s}{y} \right)_A}$ and $\overline{\left(\frac{D_s}{y} \right)_P}$ are the measured and model-estimated mean data values, respectively. The model performance was evaluated using RMSE with a range of 0 to $+\infty$ (optimum zero); generally, a low RMSE/MAPE/MPE and a high R^2 mean a more efficient model performance. The general framework for this research work is shown in figure 4.

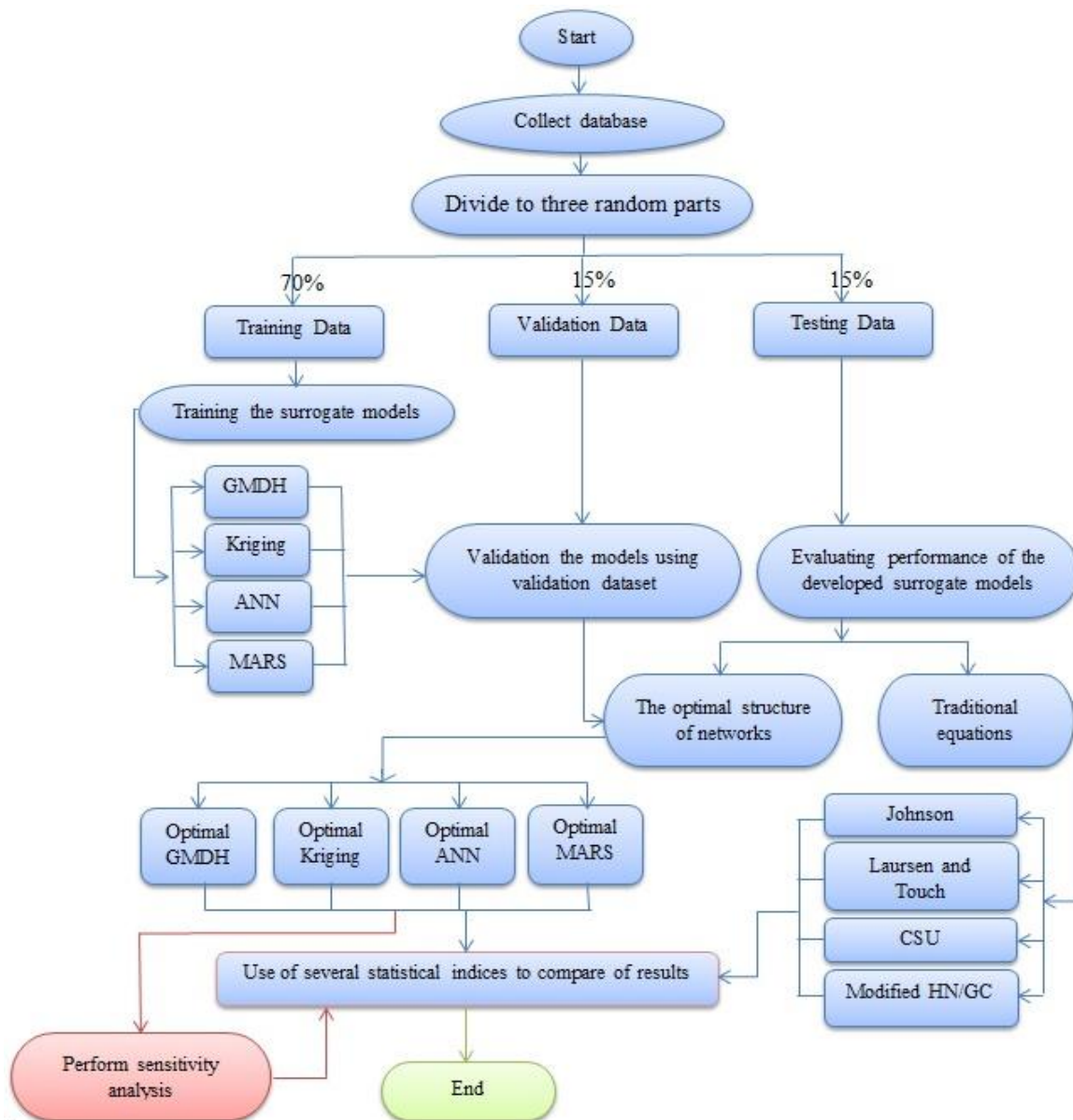


Figure 4. Research framework.

3.1. Artificial Neural Networks (ANNs)

The ANNs model is an intelligent system capable of modeling complex problems and solving complicated systems in many fields such as the optimization, prediction, estimation, and simulation. Its structure consists of some input, hidden, and output layers, each of which has a network of artificial neurons called "nodes". The nodes in the input and output layers are indications of the independent and dependent variables, respectively, and one or more hidden layers, which are neither input nor output, can constitute the ANNs network. In a layer, all the nodes send signals to interact and make links with those in the adjacent layers for the ANNs network to be fully connected. Since each node applies a typical activation function (tansig, purelin, etc.) to generate its output signal, the output variables are produced by merging the connection weights/biases with each input node after passing through an activation function. The target values ($\hat{y}(x)$) are, therefore, calculated as follows:

$$\hat{y}(x) = \sum_{i=1}^m \alpha_i \varphi(\alpha_i), \& \alpha_i = \sum_{j=1}^p w_{ij} x_j + \beta_j \quad (9)$$

where α , w , and β are the network's uncertain parameters (weights, bias terms, etc.), $\varphi(x)$ is a transfer function, m is the number of neurons in the hidden layer, and p is the number of inputs [34]. Next, the multilayered perceptron method

and back-propagation algorithm were used in order to find the optimal ANNs network structure to determine the number of hidden layers and nodes as well as the type of the activation function in each layer.

The ANNs network first uses the training dataset to train itself and then the validation dataset in order to evaluate its performance; the process continues until MSE reaches its minimum:

$$MSE = \frac{1}{n} \sum_{i=1}^n (E_i - N_i)^2 \quad (10)$$

where N_i are the measured data, E_i are the model estimation, and n is the number of data points. Thus this network, with variable hidden layers and nodes and various activation functions (tansig, purelin) is investigated until the error of the validation set is minimized and the best performance is achieved.

Figure 5 shows this work's optimal ANNs structure extracted with four neurons in the input layer corresponding to four input data $\left(F_r, \frac{b}{y}, \frac{D_{50}}{y}, \sigma \right)$. The best results were obtained after many trials and errors using the back-propagation algorithm with one hidden layer and 5 neurons and tansig and purelin as the optimal activation functions in the hidden and output layers, respectively.

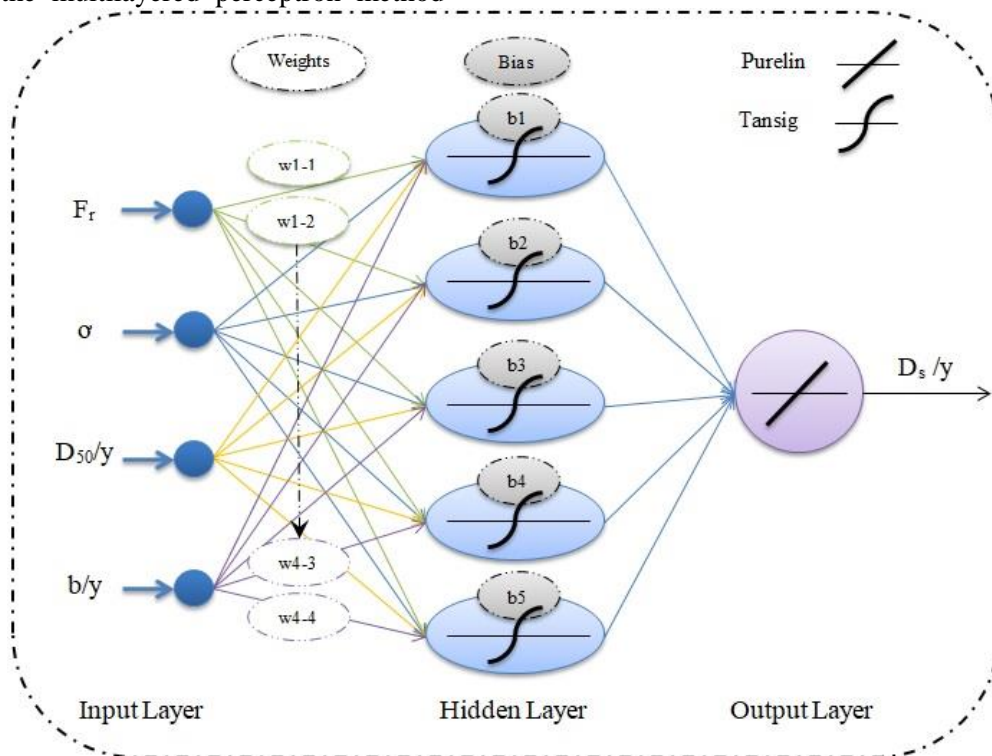


Figure 5. Final properties of the optimal ANNs model.

3.2. Group Method of Data Handling (GMDH)

First proposed by Ivakhnenko based on the principle of heuristic self-organization, GMDH is a kind of ANNs learning machine algorithm capable of being used in such various problems as the complex system modeling, function approximation, non-linear regression, pattern recognition, and so on. It presents a model as a set of neurons different pairs of which are linked in each layer through quadratic polynomials to generate new neurons in the next layer. The main objective of the identification problem is to find a good approximation function \hat{f} that can estimate the actual output \hat{y} for a given input vector $X = (x_1, x_2, \dots, x_n)$.

Thus for a given set of n samples (multi-input-single-output data pairs), we will have:

$$y_i = f(x_{i1}, x_{i2}, \dots, x_{in}) \quad (i=1, 2, \dots, m) \quad (11)$$

The GMDH model is now trained in order to estimate the target \hat{y}_i for any given input vector X as follows:

$$\hat{y}_i = \hat{f}(x_{i1}, x_{i2}, \dots, x_{in}) \quad (i=1, 2, \dots, m) \quad (12)$$

and minimizes the squared difference between the real and predicted values as:

$$E = \min \left(\sum_{i=1}^m (\hat{f}(x_{i1}, x_{i2}, \dots, x_{in}) - y_i)^2 \right) \quad (13)$$

The basic form of the GMDH algorithm (figure 6) that yielded the input-output variables relationship could, therefore, be shown by the VKG (Volterra-Kolmogorov-Gabor) polynomial transfer function as follows [35, 36]:

$$y_m = a_0 + \sum_{i=1}^n a_i x_i + \sum_{i=1}^n \sum_{j=1}^n a_{ij} x_i x_j + \sum_{i=1}^n \sum_{j=1}^n \sum_{k=1}^n a_{ijk} x_i x_j x_k \dots, \quad (14)$$

where a_0 is the bias component, $X = (x_1, x_2, \dots, x_n)$ is the vector of input variables, $A = (a_1, a_2, \dots, a_n)$ is the vector of weights, and y is the output variable in each node.

In this scenario, the network layers contain similar PD polynomial orders, and that of each neuron (PN) is kept unchanged throughout the network. For instance, if the first layer PN polynomials are quadratic:

$$\hat{y} = G(x_i, x_j) = a_0 + a_1 x_i + a_2 x_j + a_3 x_i x_j + a_4 x_i^2 + a_5 x_j^2 \quad (15)$$

Here, the network is designed with a similar procedure since all of its layers' neurons' polynomials are similar; compared to the quadratic polynomials, the tri-quadratic and 3rd-order ones form a more sophisticated network, whereas the bilinear polynomials produce less complex structures. Earlier studies have revealed that selecting polynomials may be dependent on the objective function's minimum error and the polynomial type complications. In this work, we used the quadratic polynomials to model the bridge-pier vicinity scour depth, and regression techniques in order to find the weighting coefficients in (15) to minimize the difference between y and \hat{y} (actual and calculated outputs) for each x_i, x_j pair (input variables). Hence, the weighting coefficients of the quadratic function G_i were obtained as follows to optimally fit the output in the whole set of the input-output data pair:

$$E = \frac{\sum_{i=1}^m (y_i - G_i)^2}{m} \rightarrow \min \quad (16)$$

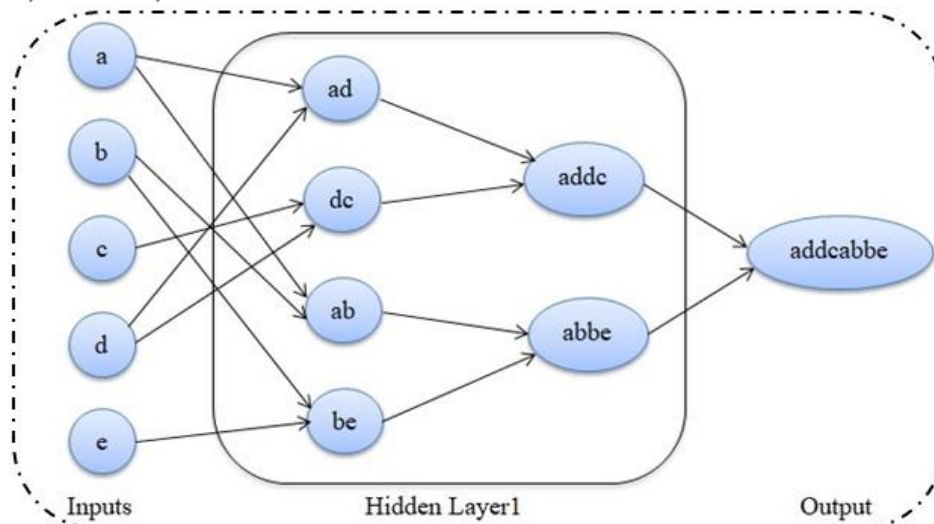


Figure 6. Schematic architecture of GMDH networks [36].

Also in order to optimize such GMDH parameters as the maximum number of neurons/layers and the selection pressure by the training/validation datasets, the trial-and-error method was used so that the network was first trained by the training dataset and was then evaluated by the validation dataset until the mean squared error was minimized to yield the best performance. In the optimal structure, the maximum number of neurons, layers, and selection pressure were found to be 14, 4 and 0.675, respectively.

3.3. Kriging Model

The Gaussian process regression or Kriging is a semi-parametric meta-modeling interpolation method that estimates, based on the known observed information, the unknown information at a point as follows [37, 38]:

$$\hat{g}(x) = F(x, \beta) = f^T(x)\beta + z(x) \quad (17)$$

where $F(x, \beta)$ (constant or polynomial) is the regression base representing the Kriging trend, $g(x)$ is supposedly the random process realization, $f(x)$ is the Kriging basis, and β is the regression coefficient. Different forms of $f^T(x)\beta$ are usually

ordinary (β_0), linear ($\beta_0 + \sum_{n=1}^N \beta_n x_n$) or quadratic ($\beta_0 + \sum_{n=1}^N \beta_n x_n + \sum_{n=1}^N \sum_{k=1}^N \beta_{nk} x_n x_k$), n is the dimension of the random input vector x , and $z(x)$ is the Kriging interpolation following a stationary Gaussian process with zero mean and a covariance matrix between the points x_i and x_j defined as follows:

$$COV(Z(x_i), Z(x_j)) = \sigma^2 R(x_i, x_j; \theta) \quad (18)$$

where σ^2 is the process variance or the generalized mean squared error from the regression part based on the best linear unbiased predictor, $R(x_i, x_j; \theta)$ is the correlation (kernel) function representing the process correlation function with hyper-parameter θ that has a significant impact on the Kriging performance.

The Kriging model used in this work was an ordinary type, and the correlation functions (linear, exponential, Gaussian, cubic, spherical, and spline) along with constant, linear, and quadratic polynomials (degree 0, 1 and 2, respectively) were evaluated in order to find the optimal model parameters. After approximating the training dataset, the model created for different functions and degrees was evaluated by the validation dataset with the MSE index. Finally, the 2nd-order and exponential functions were selected as the best approximations for the analyses.

3.4. Multivariate Adaptive Regression Splines (MARS)

A non-linear nonparametric method first introduced by Friedman, MARS defines the relationship between some sets of input-output variables in a high-dimensional data region using a group of coefficients and piecewise-defined polynomials [39].

MARS, which is a non-parametric non-linear method of developing relationships among different sets of input and dependent variables in an n-dimensional data region without requiring any special assumptions about the input variables-output underlying functional relationships, is based on a divide-and-conquer strategy wherein the training data divides into separate splines of varying slopes. Knots or segments' end points mark the end of one data region and the start of another. This enables the basis functions (plotted piecewise curves) to make the models more flexible and allow a linear function to have bends, thresholds, and other departures. A linear union of the basis functions (BFs) and their interactions can help the MARS model $f(X)$ to be formed as follows [40]:

$$f(X) = \beta_0 + \sum_{m=1}^M \beta_m \lambda_m(X) \quad (19)$$

where λ_m is a basis function; either of one spline or the product of two or more; in this work, we assumed a maximum 2nd-order function to simplify the purposes, although higher orders are also possible if the data guarantees. The least-squares method is used to estimate β , which is constant, and BFs are smooth polynomials (splines) with piecewise linear/cubic functions.

The form of a piecewise linear function is $\max(0, x-t)$. It is used for simplicity and has a knot at value t . $\max(\cdot)$ means its value is zero unless the positive part is used:

$$\max(0, x-t) = \begin{cases} x-t & x \geq t \\ 0 & \text{otherwise} \end{cases} \quad (20)$$

In order to generate BFs, MARS searches stepwise among all variables' interactions and over all possible univariate knot locations, the selection of which is by an adaptive regression algorithm. To construct a MARS model, use is made of a technique with a forward phase to add functions to find the performance improvement knots until the highest predetermined number of terms are found and an intentionally over-fitted model is obtained, and a backward phase that eliminates the most ineffective terms to prevent overfitting using the GCV (Generalized Cross-Validation) method, which is a goodness of fit test

that fines for excess BFs and lessens the overfitting chance. The GCV equation for a set of training data with N observations is as follows [41]:

$$GCV = \frac{\frac{1}{N} \sum_{i=1}^N [y_i - f(x_i)]^2}{\left[1 - \frac{M + d \times (M - 1) / 2}{N}\right]^2} \quad (21)$$

where M is the number of BFs, N shows the number of observations, $f(x_i)$ are the MARS model's estimated values, and d is the fine parameter (cost per basis function optimization to make the procedure smooth. Its larger values mean fewer knots, and hence, less fluctuating estimates. Since Friedman [39] has suggested $2 \leq d \leq 4$, preferably 3 as an optimum value, (this research work has taken $d = 3$).

Equation (19) is minimized when a basis function is omitted at each step so that a good and acceptable fitting model is yielded. Since BF and the variable knot location selection are both data-based and problem-specific, MARS is considered as an adaptive procedure.

In the data-driven MARS modeling, ANOVA (analysis of variance) decomposition is used in order to evaluate the input variables' contributions and BFs by testing and comparing variables for statistical significance by placing all BFs with one variable in one group and all those with pairwise interactions (or higher when applicable) in another after the optimal MARS model has been determined.

4. Results and Discussion

4.1. Optimal Structure of Surrogate Models

In this section, we evaluate the performance of the surrogate models by plotting actual non-dimensional scour depths (D_s/y) against the estimated values. Table 4 and figures 7-11 illustrate the performance and results of the optimized ANNs, GMDH, Kriging, and MARS models for training and validation datasets. The RMSE, R^2 , MAPE, and MPE statistical parameters obtained from (5)-(8) are compared to evaluate the performance of these methods.

According to the results obtained, all the surrogate models estimated D_s/y acceptably for the training and validation datasets. The regression lines had good R^2 values (0.897-0.9997) for the training set but slightly smaller values (0.852-0.990) for the validation set; Kriging and MARS had, respectively, the higher and lower values in both cases.

A comparison of the RMSE, MAPE, and MPE statistical indicators showed that in the training part, they were lower for the Kriging model (0.0070%, 0.002%, and 10.7%) and higher for the MARS model (0.122%, 0.144%, and 81.1%). The same was the case in the validation part but with different values; (0.0033%, 0.047%, and 17.2%) for Kriging and (0.129%, 0.162%, and 40.6%) for MARS models.

A results review showed that among all the models, the optimized Kriging had the highest R^2 and the lowest RMSE, MAPE, and MPE, and contrary to other models, all its estimated values were within an accuracy range of -20% to +20% (figure 9).

According to figure 11, the values estimated in both the training and validation sets had trends similar to the actual values.

Table 4. Performance of surrogate models in the training and validation sets.

Models	Dataset	Number of data	R ²	RMSE	MAPE	MPE (%)
GMDH	Train	172	0.951	0.085	0.108	68.8
	Validation	37	0.956	0.068	0.1	30.1
Kriging	Train	172	0.9997	0.007	0.002	10.7
	Validation	37	0.990	0.033	0.047	17.2
MARS	Train	172	0.897	0.122	0.144	81.1
	Validation	37	0.852	0.129	0.162	40.6
ANNs	Train	172	0.979	0.055	0.066	27.3
	Validation	37	0.988	0.035	0.06	20.9

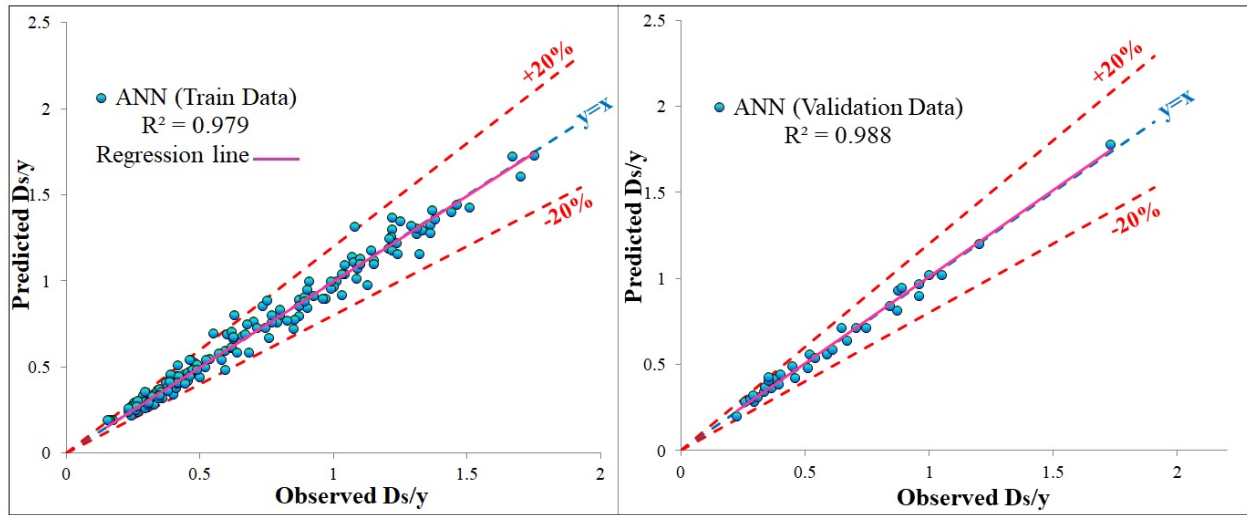


Figure 7. Performance evaluation of ANNs model developed for the training and validation sets.

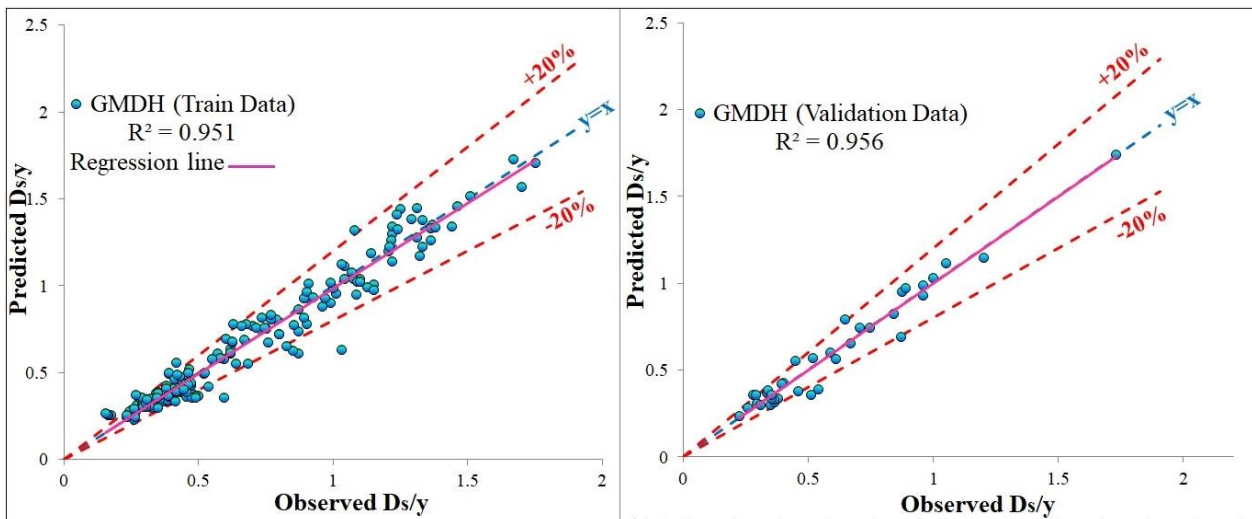


Figure 8. Performance evaluation of GMDH model developed for the training and validation sets.

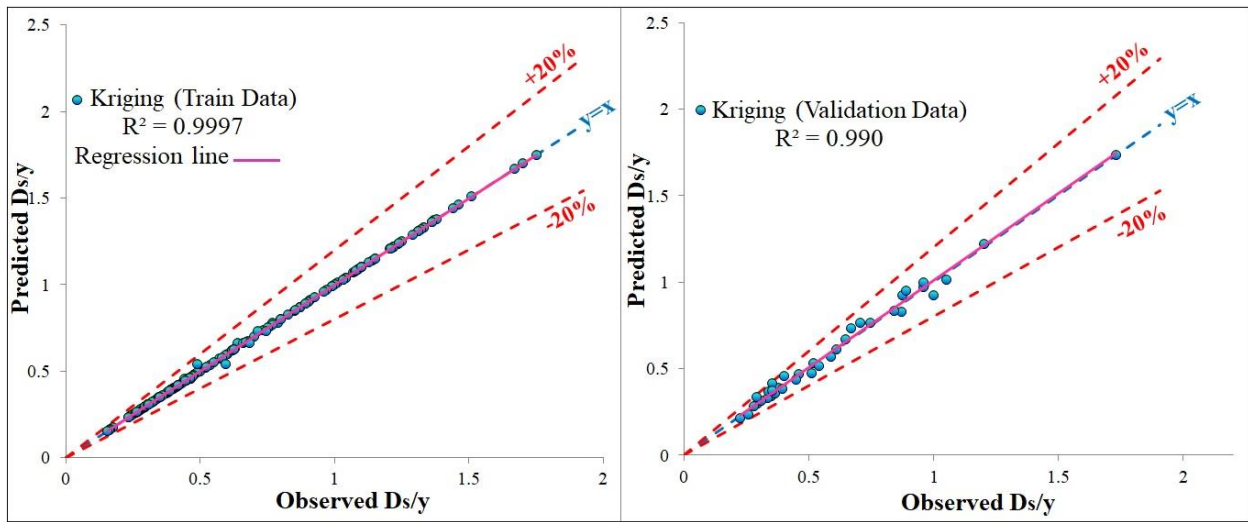


Figure 9. Performance evaluation of Kriging model developed for the training and validation sets.

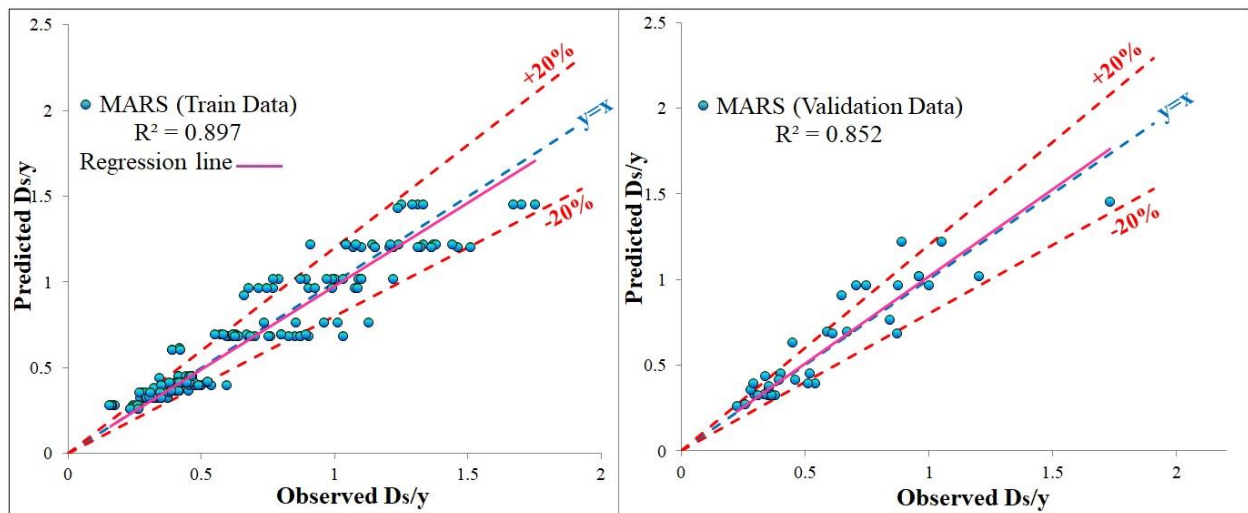


Figure 10. Performance evaluation of MARS model developed for the training and validation sets.

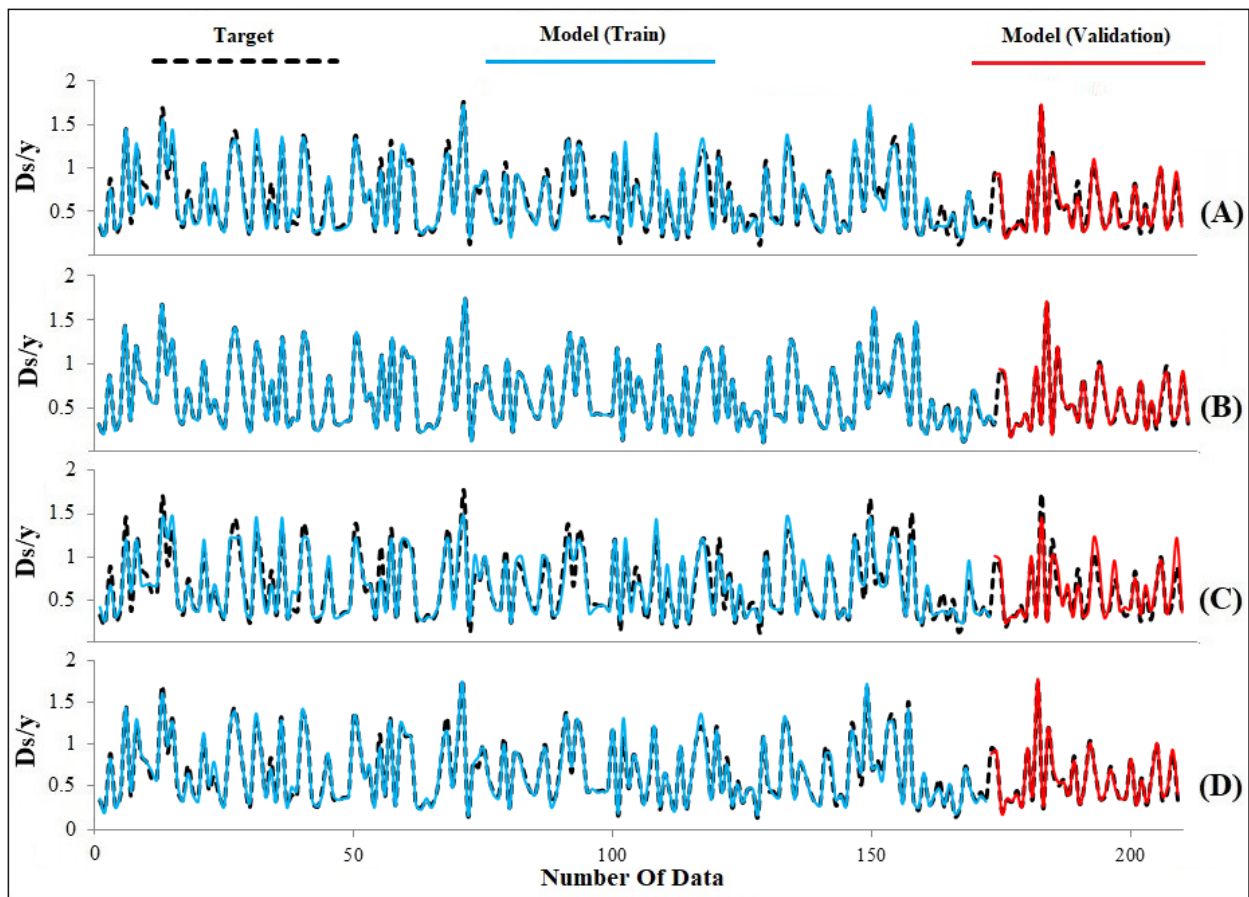


Figure 11. Schematic comparison of the optimal networks estimated in the training and validation sets: (A) GMDH, (B) Kriging, (C) MARS, and (D) ANNs.

4.2. Performance Evaluation of Developed Surrogate Models

In the previous sections, the surrogate models were developed using the training and validation datasets but this section is aimed to use the test dataset in order to evaluate the performance of the developed models through a comparison with the results of some traditional equations.

The optimal structures extracted from GMDH, Kriging, MARS, and ANNs were used to estimate D_s/y for the test dataset, and the results obtained were compared with those of the modified

HN/GC (2016), Laursen-Toch (1956), Johnson (1992), and FHWA HEC-18 (1993) empirical equations. Figures 12-15 and table 5 compare the surrogate models and traditional equations in estimating D_s/y for the test dataset, and conclude that the former did the estimation more accurately than the latter; Kriging and ANNs had better estimates than GMDH and MARS. Kriging with $R^2 = 0.947$, RMSE = 0.065, MAPE = 0.067, and an MPE of 25.1% performed the best compared to the other models.

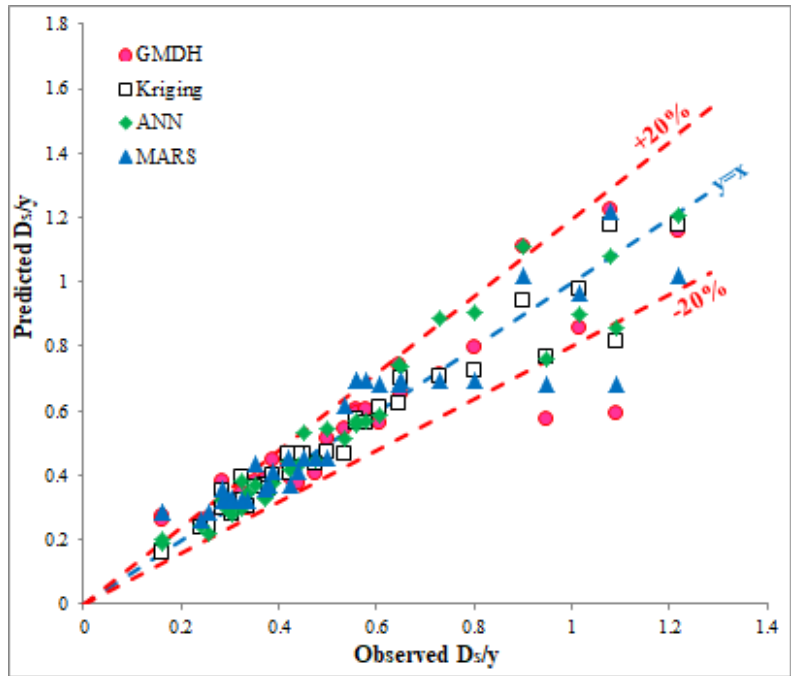


Figure 12. Comparison between the observed and computed D_s/y values by surrogate models.

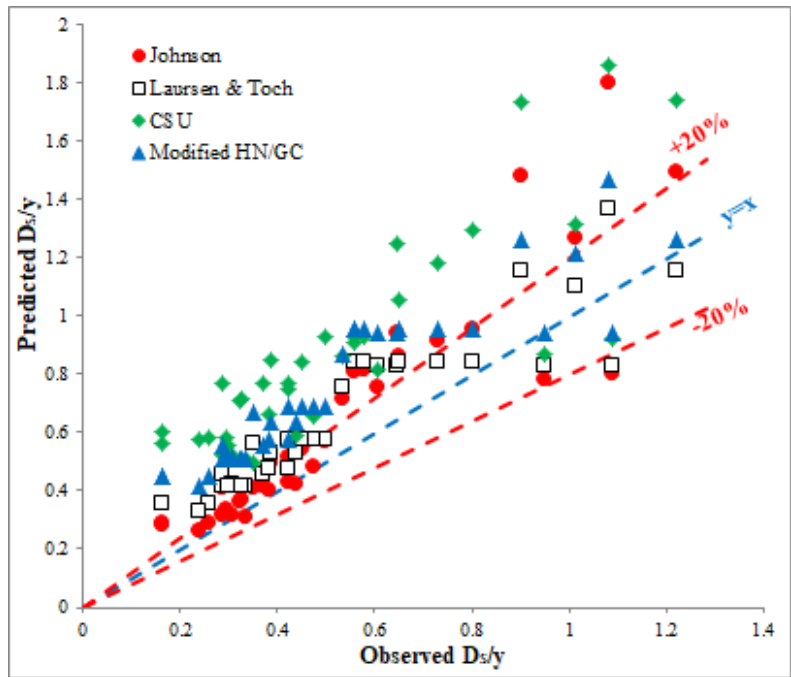


Figure 13. Comparison between the observed and computed D_s/y values by empirical equations.

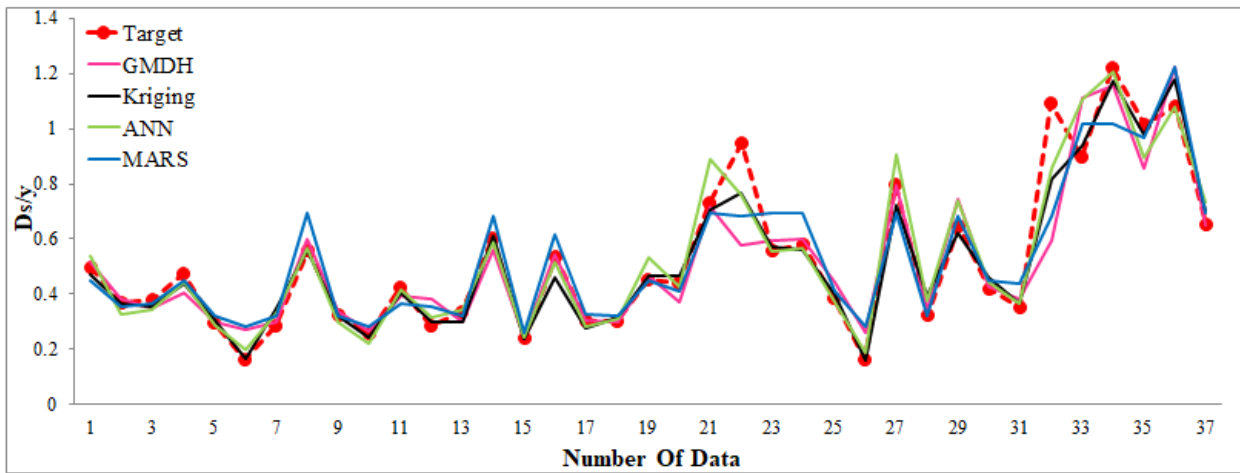


Figure 14. Estimation accuracy of the test dataset by surrogate models.

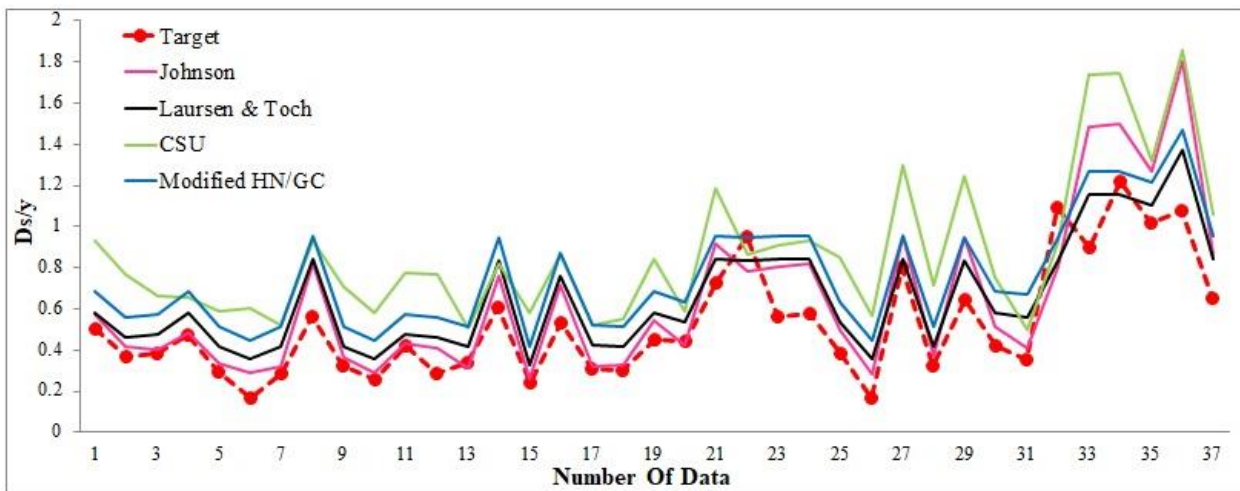


Figure 15. Estimation accuracy of the test dataset by empirical equations.

Although the empirical methods used in this work had a reasonable R^2 , their RMSE, MAPE, and MPE rates were much higher, leading to conservative results and overestimated D_s/y . Figures 12-13 show that most surrogate models' estimated values are in the -20% to +20% accuracy range, and most values obtained from the empirical equations are beyond this range. According to table 5, the highest D_s/y were overestimated by 85.3 and 58.8% (MAPE), on

average, for CSU and modified HN/GC, respectively, and the RMSE and MPE for CSU were 0.393 and 269.8%, respectively. However, the Johnson and Laursen-Toch equations had reasonable results for this test dataset compared to the mentioned equations. All in all, the statistical parameters show that the surrogate models' estimation performance is satisfactory compared to the traditional methods.

Table 5. Performance indices of various D_s/y estimation methods.

	Models	Type of data	Number of data	R^2	RMSE	MAPE	MPE (%)
surrogate models	GMDH	Test	37	0.803	0.121	0.125	65.5
	Kriging	Test	37	0.947	0.065	0.067	25.1
	Mars	Test	37	0.839	0.11	0.149	72.8
	ANNs	Test	37	0.919	0.078	0.094	22.9
empirical equations	Johnson (1992)	Test	37	0.781	0.211	0.257	77.4
	Laursen and Toch (1956)	Test	37	0.826	0.166	0.356	120.3
	CSU (1993)	Test	37	0.713	0.393	0.853	269.8
	HN/GC (2016)	Test	37	0.795	0.254	0.588	175.6

5. Sensitivity Analysis

The importance of each input variable and its effects on the surrogate model outputs were checked by the sensitivity analysis, which is, in fact, a fundamental modeling tool for a proper model application since it enables the user to find the relative importance of the input parameters and consider the effects of their errors on the model output. In this analysis, one input variable of (4) was deleted each time to evaluate its effect on the output [42].

In this research work, we analyzed the sensitivity of the estimated D_s/y to the input variables in the GMDH, Kriging, MARS, and ANNs models, extracted the optimal structure of each model based on the inputs of each scenario and the training and validation datasets, and used the test dataset in order to evaluate the performance of each scenario (tables 6 and 7).

Table 6. Sensitivity analysis results for the parameters in (4).

Scenarios	Models	Dataset	Number of data	R ²	RMSE	MAPE	MPE (%)	
$D_s/y = f(F_1, \sigma, D_{sp}/y)$	GMDH	Train	172	0.379	0.301	0.399	283.3	
		Validation	37	0.44	0.242	0.399	127	
		Test	37	0.415	0.22	0.388	132.1	
	Kriging	Train	172	0.8564	0.1446	0.1156	80.95	
		Validation	37	0.483	0.238	0.284	119.3	
		Test	37	0.733	0.163	0.269	73.2	
	Mars	Train	172	0.171	0.348	0.513	216.6	
		Validation	37	0.213	0.299	0.555	199	
		Test	37	0.241	0.279	0.595	159.9	
	ANNs	Train	172	0.813	0.165	0.19	78.4	
		Validation	37	0.747	0.163	0.196	77.4	
		Test	37	-3.66	2.846	1.072	3235.5	
	$D_s/y = f(F_1, \sigma, b/y)$	GMDH	Train	172	0.952	0.084	0.109	67.5
			Validation	37	0.955	0.07	0.106	30.3
			Test	37	0.811	0.119	0.13	60.2
Kriging		Train	172	0.9997	0.0066	0.0022	10.71	
		Validation	37	0.982	0.045	0.062	37.9	
		Test	37	0.834	0.111	0.093	43.2	
Mars		Train	172	0.897	0.122	0.144	81.1	
		Validation	37	0.852	0.129	0.162	40.6	
		Test	37	0.839	0.11	0.149	72.8	
ANNs		Train	172	0.971	0.066	0.085	54.5	
		Validation	37	0.986	0.039	0.066	24.4	
		Test	37	0.828	0.114	0.128	47.7	

Table 7. Sensitivity analysis results for the parameters in (4).

Scenarios	Models	Dataset	Number of data	R ²	RMSE	MAPE	MPE (%)
$D_s/y = f(F_r, D_{50}/y, b/y)$	GMDH	Train	172	0.952	0.084	0.111	64.9
		Validation	37	0.963	0.063	0.102	30.3
		Test	37	0.803	0.122	0.136	58.9
	Kriging	Train	172	0.9997	0.0066	0.0022	10.71
		Validation	37	0.983	0.046	0.067	26.5
		Test	37	0.882	0.096	0.086	35.7
	Mars	Train	172	0.897	0.122	0.144	81.1
		Validation	37	0.852	0.129	0.162	40.6
		Test	37	0.839	0.11	0.149	72.8
	ANNs	Train	172	0.992	0.035	0.051	43.6
		Validation	37	0.973	0.056	0.078	22.2
		Test	37	0.917	0.079	0.099	36.1
$D_s/y = f(\alpha, D_{50}/y, b/y)$	GMDH	Train	172	0.914	0.112	0.129	60.6
		Validation	37	0.901	0.116	0.159	45.5
		Test	37	0.838	0.11	0.134	43.5
	Kriging	Train	172	0.9679	0.0684	0.0573	33.85
		Validation	37	0.935	0.086	0.078	36.9
		Test	37	0.927	0.075	0.076	23.6
	Mars	Train	172	0.897	0.122	0.144	81.1
		Validation	37	0.852	0.129	0.162	40.6
		Test	37	0.839	0.11	0.149	72.8
	ANNs	Train	172	0.956	0.08	0.081	38.7
		Validation	37	0.946	0.077	0.094	34.8
		Test	37	0.924	0.077	0.094	38.8

In scenario 1, D_s/y was assumed to be a function of F_r , α , and D_{50}/y ; all the surrogate models yielded a very poor estimation of D_s/y in the test dataset (table 6), concluding that the assumed input variables had a low modeling importance. In this scenario, ANNs performed the worst in the test dataset despite its slightly reasonable performance in estimating the training and validation datasets. Overall, herein the Kriging model has had the best performance among all models.

In scenario 2, D_s/y was assumed to be a function of F_r , α , and b/y ; all the surrogate models yielded better results than scenario 1 (table 6). In general, all models had a similar performance, Kriging was slightly better, and MARS was slightly worse in the training and validation datasets.

In scenario 3, the non-dimensional scour depth was assumed to be a function of F_r , D_{50}/y , and b/y decision variables (table 7). All the surrogate models performed reasonably but ANNs and Kriging were better than the others.

In the last scenario, α , D_{50}/y , and b/y were defined as the model input parameters (table 7). As shown

in tables 6 and 7, this scenario had the best performance compared to the others; Kriging and ANNs performed better but the MARS performance was exactly the same as in scenario 3.

Finally, the sensitivity analyses showed that among the variables in (4), non-dimensional b/y had the highest and F_r and α had the least effect on the estimated normalized local scour depth (D_s/y) for all models according to the definition of database under live bed conditions with a uniform sediment and a sub-critical flow regime.

6. Comparison with Related Works

Since each earlier similar work is based on some data gathered from databases different in terms of scales and water flow/sediment statistical/hydraulic characteristics, a fair precise comparison is almost impossible. However, the results of the present work are presented in table 8 along with those of some other related works most of which are mentioned in the “Introduction”.

Table 8. Comparison of the results of this study with those of some previous works.

Source	Data type	Number of data	Reviewed models	Comparison with empirical formula	Selected model	Most influential parameter (sensitivity analysis)
Batani et al. [7]	Laboratory data	263	ANNs methods (MLP/BP & RBF/OLS) & ANFIS (adaptive neuro-fuzzy inference system)	Yes	ANN (MLP/BP)	pier diameter
Firat and Gungor [14]	Laboratory data	165	Generalized Regression Neural Networks (GRNN) and Feed Forward Neural Networks (FFNN)	Yes	GRNN	pier dimension and grain size
Najafzadeh et al. [15]	Laboratory data	95	GMDH	Yes	GMDH	clay percentage (cohesive bed material)
Batani et al. [8]	Laboratory data	347	Genetic expression programming (GEP) and MARS	Yes	MARS	pile diameter
Azamathulla et al. [19]	Field data	398	Genetic programming (GP) and ANNs	Yes	GP	-
Najafzadeh [43]	Laboratory data	321	NF-GMDH-PSO and NF-GMDH-GSA	Yes	NF-GMDH-PSO	pier diameter
This study	Laboratory data	246	ANN, GMDH, MARS and Kriging	Yes	Kriging	pier diameter

As mentioned earlier, the model inputs (table 8) have been gathered from different references under different water flow/sediment conditions, and have different statistical characteristics and distributions. However, the deduction from table 8 is that the alternative models in all the mentioned references had performed better than the experimental relationships, and the index related to the bridge pier-section shape-dimension parameter, in most references, had the greatest impact on the outputs of different models. However, this work that has compared the Kriging model performance with those of the GMDH, ANNs, MARS and some existing traditional equations, shows the Kriging model's efficiency and reveals that it can have an acceptable performance in estimating the bridge-pier scour depth.

7. Summary and Conclusions

In this work, we investigated four surrogate models, namely artificial neural networks (ANNs), group method of data handling (GMDH), multivariate adaptive regression splines (MARS), and Gaussian process models (Kriging) that use the non-dimensional decision variables in order to estimate the local scour depth at circular piers. The optimal structure of each model was extracted with the training and validation datasets, and comparison of their statistical indicators showed that Kriging and MARS, respectively, had the highest and lowest precision in the D_s/y estimation among the other surrogate models.; according to this comparison, the statistical

indicators in the training dataset showed that Kriging and MARS had RMSE, MAPE, and MPEs equal to 0.0070%, 0.002%, and 10.7%, and 0.122%, 0.144%, and 81.1%, respectively.

Then the testing dataset was used in order to evaluate the performance of these methods through a comparison with four empirical equations, namely Laursen-Toch (1956), Johnson (1992), CSU (1993), and modified HN/GC (2016). The results obtained showed that all methods were good enough to estimate D_s/y with the dataset used in this work but the traditional equations led to conservative and overestimated results. Most of the values estimated by the surrogate models were within the -20% to +20% accuracy range, and most of those estimated by the empirical formulas were beyond this range, concluding that all the surrogate models estimated the non-dimensional local scour depth (D_s/y) much more accurately than the empirical equations. Among all the tested surrogate models, Kriging and ANNs had the highest match to the target values with the RMSE, MAPE, MPE, and R^2 statistical indicators of 0.065, 0.067, 25.1%, and 94.7%, and 0.078, 0.094, 22.9% and 91.9%, respectively. Finally, the results obtained showed that Kriging had the best estimations in all the three parts (training, validation, and test datasets), concluding that it was the most robust among all models.

The sensitivity of the estimated local scour depth (D_s/y) to the approach flow Froude number (F_r), sediment gradation coefficient (σ), pier width-to-flow depth ratio (b/y), and ratio of average

sediment size-to-flow depth ratio (D_{50}/y) was analyzed, and the results obtained showed that (b/y) was the most effective parameter in the normalized scour depth (D_s/y) for all the surrogate models, and F_r and σ had the least effects on the estimations.

References

- [1] A.M. Shirhole and R.C. Holt, "Planning for a comprehensive bridge safety program," *Transportation Research Record*, vol. 1290, pp.39-50, 1999.
- [2] H.N.C. Breusers, G. Nicollet and H.W. Shen, "Local scour around cylindrical piers," *Journal of Hydraulic Research*, vol. 15, pp. 211–252, Jun 1977.
- [3] B.W. Melville and S.A. Coleman, "Bridge Scour," Water Resources Publications, Highlands ranch, Colorado, USA, 2000.
- [4] E.V. Richardson and S.R. Davis, "Evaluating scour at bridges, Hydraulic Engineering Circular no. 18," FHWA NHI, Washington DC, USA, Rep. FHWA NHI, 2001.
- [5] D.M. Sheppard and Jr. W. Miller, "Live-bed local pier scour experiments," *Journal of Hydraulic Engineering*, vol. 132, pp. 635–642, July 2006.
- [6] R. Ettema, B.W. Melville and B. Barkdoll, "Scale effect in pierscours experiments," *Journal of Hydraulic Engineering*, vol. 124, pp. 639–642, 1998.
- [7] S.M. Bateni, S.M. Borghei and D.S. Jeng, "Neural network and neuro-fuzzy assessments for scour depth around bridge piers," *Engineering Applications of Artificial Intelligence*, vol. 20, pp. 401–414, April 2007.
- [8] S.M. Bateni, H.R. Vosoughifar, B. Truce and D.S. Jeng, "Estimation of Clear-Water Local Scour at Pile Groups Using Genetic Expression Programming and Multivariate Adaptive Regression Splines," *Journal of Waterway, Port, Coastal, and Ocean Engineering*, vol. 145, pp. 04018029, January 2019.
- [9] R.V. Raikar, C.Y. Wang, H.P. Shih and J.H. Hong, "Prediction of contraction scour using ANN and GA," *Flow Measurement and Instrumentation*, vol. 50, pp. 26–34, 2016.
- [10] Q. Zhang, X.L. Zhou and J.H. Wang, "Numerical investigation of local scour around three adjacent piles with different arrangements under current," *Ocean Engineering*, vol. 142, pp. 625–638, September 2017.
- [11] Y. Hassanzadeh, A. Jafari-Bavil-Olyaei, M.T. Aalami and N. Kardan, "Experimental and numerical investigation of bridge pier scour estimation using ANFIS and teaching-learning-based optimization methods," *Engineering with Computers*, vol. 35, pp. 1103-1120, October 2018.
- [12] N.M. Dang, D.T. Anh and T.D. Dang, "ANN optimized by PSO and Firefly algorithms for predicting scour depths around bridge piers," *Engineering with Computers*, vol. 18, pp. 1-11, July 2019.
- [13] M. Fatahi and B. Lashkar-Ara, "Estimating scour below inverted siphon structures using stochastic and soft computing approaches," *Journal of AI and Data Mining*, vol. 5, pp. 55–66, October 2016.
- [14] M. Firat and M. Gungor, "Generalized regression neural networks and feed forward neural networks for prediction of scour depth around bridge piers," *Advances in Engineering Software*, vol. 40, pp. 731–737, August 2009.
- [15] M. Najafzadeh, G.A. Barani and H.M. Azamathulla, "GMDH to predict scour depth around a pier in cohesive soils," *Applied Ocean Research*, vol. 40, pp. 35–41, March 2013.
- [16] S. Qin, Y.L. Zhou, H. Cao and M.A. Wahab, "Model Updating in Complex Bridge Structures using Kriging Model Ensemble with Genetic Algorithm," *KSCE Journal of Civil Engineering*, vol. 22, pp. 3567-3578, November 2017.
- [17] X. Fan, P. Wang and F. Hao, "Reliability-based design optimization of crane bridges using Kriging-based surrogate models," *Structural and Multidisciplinary Optimization*, vol. 59, pp. 993-1005, January 2019.
- [18] P. Lu, Z. Xu, Y. Chen and Y. Zhou, "Prediction method of bridge static load test results based on Kriging model Pengzhen," *Engineering Structures*, vol. 214, pp. 110641, July 2020.
- [19] H.M. Azamathulla, A.A. Ghani, N.A. Zakaria and A. Guven, "Genetic programming to predict bridge pier scour," *Journal of Hydraulic Engineering*, vol. 136, pp. 165–169, March 2010.
- [20] M. Najafzadeh and H.M. Azamathulla, "Neuro-fuzzy GMDH systems to predict the scour pile groups due to waves," *Journal of Computing in Civil Engineering*, vol. 29, pp. 04014068, 2013.
- [21] N. Ghaemi, A. Etemad-Shahidi and B. Ataie-Ashtiani, "Estimation of current- induced pile groups scour using a rule based method," *Journal of Hydroinformatics*, vol. 15, pp. 516–528, 2013.
- [22] A.M. Sattar, "Gene expression models for the prediction of longitudinal dispersion coefficients in transitional and turbulent pipe flow," *Journal of Pipeline Systems Engineering and Practice*, vol. 5, pp. 04013011, February 2014.
- [23] H. Shan, R. Kilgore, J. Shen and K. Kerenyi, "Updating HEC-18 Pier Scour Equations for Noncohesive Soil," United States, Federal Highway Administration, Office of Infrastructure Research and Development, 2016.
- [24] E.M. Laursen and A. Toch, "Scour around bridge piers and abutments," Ames, IA: Iowa Highway Research Board, 1956.

- [25] P.A. Johnson, "Reliability-based pier scour engineering," *Journal of Hydraulic Engineering*, vol. 118, pp. 1344–1358, Jan 1992.
- [26] E.V. Richardson, L.J. Harrison, J. Richardson and S. Davis, "Evaluating scour at bridges (No. HEC 18 (2nd edition)), Administration (FHWA), Washington, D.C, 1993.
- [27] Y.M. Chiew, "Local Scour at Bridge Piers," School of Engineering, The Univ. of Auckland, Auckland, New Zealand, Rep. 355, 1984.
- [28] J. Chabert and P. Engeldinger, "Etude des affouillements autor des piles de ponts," Chatou, Rep. Natl. Hydraul Lab., 1956.
- [29] R.K. Chee, "Live-bed scour at bridge piers," Auckland University, New Zealand, Rep. 290, 1982.
- [30] S.C. Jain and E.E. Fischer, "Scour around bridge piers at high Froude numbers," Federal Highway Administration, U.S. Department of Transportation, Washington, D.C, 1979.
- [31] S.C. Jain and E.E. Fischer, "Scour around bridge piers at high flow velocities" *Journal of Hydraulic Engineering*, vol. 106, pp. 1827–1842, 1980.
- [32] A.H. Chen, "Local scour around circular piers," Ph.D. dissertation, Asian Institute of Technology, Bangkok, Thailand, 1980.
- [33] B.W. Melville and A.J. Sutherland, "Design method for local scour at bridge piers," *Journal of Hydraulic Engineering*, vol. 114, pp. 1210-1226, October 1988.
- [34] A.J. Keane and P.B. Nair, "Computational approaches for aerospace design: the pursuit of excellence" John Wiley&Sons, Ltd, West Sussex 582, 2005.
- [35] A.G. Ivakhnenko, "The group method of data handling in prediction problems," *Soviet Automatic Control*, vol. 9, pp. 21-30, 1976.
- [36] G.C. Onwubolu, "GMDH-methodology and implementation in MATLAB," London: Imperial College Press, 2016.
- [37] J. Sacks, W.J. Welch, T.J. Mitchell and H.P. Wynn, "Design and analysis of computer experiments," *Statistical Science*, vol. 1, pp. 409–423, 1989.
- [38] D.R. Jones, "A taxonomy of global optimization methods based on response surfaces," *Journal of Global Optimization*, vol. 21, pp.345–383, December 2001.
- [39] J.H. Friedman, "Multivariate adaptive regression splines," *Annals of Statistics*, vol. 1, pp. 1–67, 1991.
- [40] W. Zhang, "MARS Applications in Geotechnical Engineering Systems," Springer Nature Customer Service Center LLC, 2020.
- [41] T. Hastie, R. Tibshirani and J. Friedman, "The elements of statistical learning," Springer New York, New York, 2009.
- [42] R.H. McCuen, "Modeling Hydrologic Change: Statistical Methods," Lewis Publishers CRC Press, Boca Raton, 2016.
- [43] M. Najafzadeh, "Neuro-fuzzy GMDH systems based evolutionary algorithms to predict scour pile groups in clear water conditions," *Ocean Engineering*, vol. 99, pp. 85-94, May 2015.

تخمین عمق آبشویی پایه: مقایسه روابط تجربی با روش های ANNs، GMDH، MARS و Kriging

مسلم زربازو سیاهکلی^۱، عباسعلی قادری^۱، عبدالحمید بحرپیما^{۱*}، محسن راشکی^۲ و ناصر صفائیان حمزه کلانی^۳

^۱ گروه مهندسی عمران، دانشگاه سیستان و بلوچستان، زاهدان، ایران.

^۲ گروه مهندسی معماری، دانشگاه سیستان و بلوچستان، زاهدان، ایران.

^۳ گروه مهندسی عمران، دانشگاه بزرگمهر قائن، قائن، ایران.

ارسال ۲۰۲۰/۰۹/۲۶؛ بازنگری ۲۰۲۰/۱۰/۲۷؛ پذیرش ۲۰۲۰/۱۲/۲۱

چکیده:

آبشستگی هنگامی رخ می‌دهد که جریان آب، مواد بستر اطراف سازه پایه پل را مورد شستشو قرار دهد، که این پدیده، مساله‌ای جدی در ارزیابی ایمنی پل‌ها می‌باشد. لذا به منظور تخمین عمق آبشستگی اطراف پایه پل، روابط و مدل‌های مختلفی تاکنون ارائه گردیده است. در این مقاله توانایی تخمین عمق آبشستگی اطراف پایه دایره‌ای شکل، با استفاده از مدل‌های جایگزین در مقایسه با روابط تجربی معمول، مورد بررسی واقع شده است. بدین منظور عمق آبشستگی پایه، در خاک غیرچسبنده با شرایط جریان زیربحرانی و شرایط جریان آب و رسوب بستر پویا با استفاده از مدل‌های ANN، GMDH، MARS و Kriging تخمین زده شده است. لذا از یک پایگاه داده آزمایشگاهی شامل ۲۴۶ داده، که از مطالعات مختلف جمع‌آوری گردیده به منظور ساخت مدل‌های جایگزین استفاده گردید. این مجموعه داده به سه بخش تصادفی به نام‌های (۱) آموزش (۲) اعتبارسنجی و (۳) تست تقسیم و در ادامه نیز، از معیارهای آماری همچون ضریب تعیین (R^2)، جذر میانگین مربعات خطا (RMSE)، درصد میانگین مطلق خطا (MAPE) و میانگین درصد خطا (MPE) به منظور مقایسه نتایج این مدل‌ها در برابر برخی از فرمول‌های تجربی مرسوم استفاده شد. نتایج بدست آمده بیانگر دقت تخمین بهتر مدل‌های جایگزین در مقایسه با روابط تجربی بوده و از بین مدل‌های مورد بررسی نیز، مدل Kriging بهترین تخمین را داشته است. همچنین تحلیل حساسیت این مدل‌ها نشان داد که، عبارت بی بعد مرتبط با عرض پایه (b/y) بیشترین تاثیر را در تخمین عمق بی بعد آبشستگی (D_s/y) داشته است.

کلمات کلیدی: آبشستگی پایه، مدل‌های جایگزین، شبکه‌های عصبی مصنوعی، کریجینگ، تحلیل حساسیت.